RSC Advances

SUPPORTING INFORMATION

Design of bright near-infrared-emitting quantum dots capped with different stabilizing ligands for tumor targeting

Received 00th September 2017,
Accepted 00th September 2017

DOI:

www.rsc.org/

Xijing Liu,[a] Peijiang Zhou,*[a] Hongyu Liu,[a] Hongju Zhan,[b] Qiang Zhang[c] Yanan Zhao[c] and Yun Chen*[c]

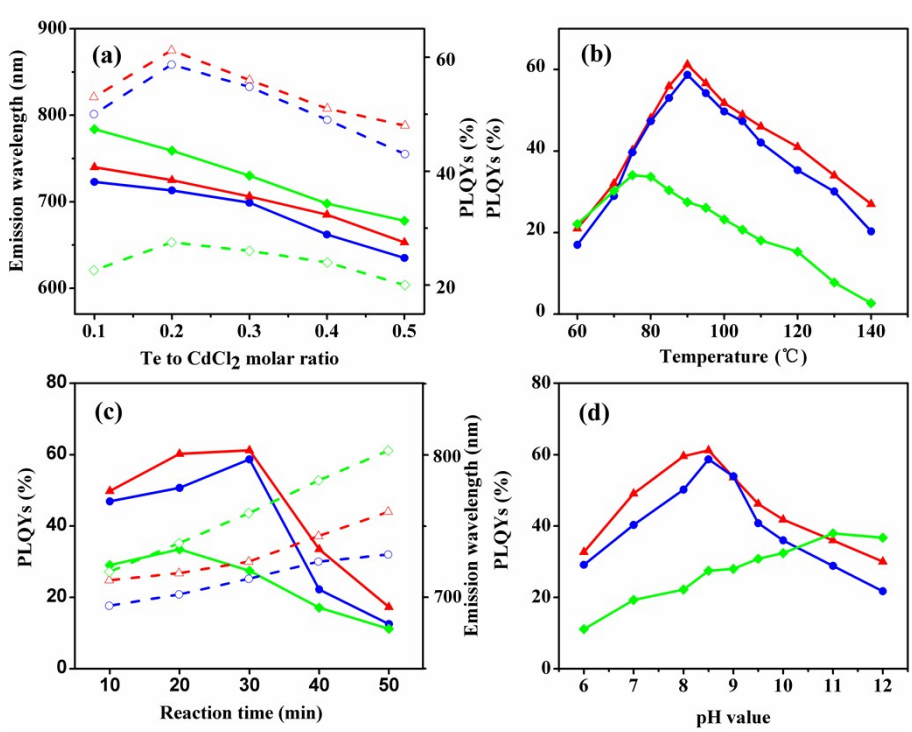

Fig. S1 (a) Emission wavelength (solid lines) and PLQYs (dashed lines) of CdHgTe/CdS /CdZnS QDs versus different molar ratios between Te and $CdCl_2$ in precursor solution. (b) PLQYs of CdHgTe/CdS/CdZnS QDs during their growth at different temperatures. (c) PLQYs (solid lines) and emission wavelength (dashed lines) of CdHgTe/CdS/CdZnS QDs during their growth at different reaction time. (d) PLQYs of CdHgTe/CdS/CdZnS QDs versus different pH values of initial precursor solutions. For all samples, emission features of selected NAC (blue), MPA (red) and TGA (green) capped CdHgTe/CdS/CdZnS QDs, respectively.

The formation of core-shell-shell (CSS) QDs would lead to a red shift in both UV-vis absorption and PL spectrum because of the lower band-gap energy of shells.[1] The traditional method of synthesizing core-shell-shell QDs usually involves three separate steps: (I) synthesis of core QDs. (II) coating of other reactants on the core with various thicknesses of shell. (III) purifying the solution and coating of other reactants on the core/shell QDs with lower band-gap energy of shell. Dispute these fussy

[a] School of Resource and Environmental Science, Hubei Biomass-Resource Chemistry and Environmental Biotechnology Key Laboratory, Wuhan University, Wuhan 430079, China
[b] Jingchu University of Technology, Jingmen 448000, China
[c] Department of Biomedical Engineering, School of Basic Medical Sciences, Wuhan University, Wuhan 430071, China
E-mail: 2013102050031@ whu.edu.cn

progresses, the extent of the shell thickness on the optical properties of aqueous core-shell QDs has not yet been well controlled, which always results in the decline of the PLQYs.[1] Thus, we used miraculous program process of microwave irradiation (PPMI) to synthesis CdHgTe/CdS QDs via one-pot route.[2] To further enhance the PLQYs and improve the biocompatibility, a CdZnS shell was epitaxially overcoated around the outer layer of the CdHgTe/CdS CS QDs to form the CdHgTe/CdS/ CdZnS CSS QDs. We found that the Te^{2-} to $CdCl_2$ molar ratio is the key factor during the formation of the CdS shell whether the thiols changed. The result of Fig. S2a revealed the trend of the PL emission peak shifting to longer wavelength was due to the gradually reductive Te content in the CdHgTe/CdS/CdZnS QDs. Therefore, when the $[Te^{2-}]$ / $[CdCl_2]$ < 0.4, the thiol ions, which originate from NAC, MPA or TGA, are believed to react with massive free Cd^{2+} ions to form the thiol-binding cadmium complexes, which resulted in red shift of PL spectrum and high PLQYs.[2,3] As for NAC-capped QDs, the PLQYs was gradually enhanced and up to 59.2% while the $[Te^{2-}]$ / $[CdCl_2]$ ratio reached the optimum value of 0.2. However, the PLQY was decreased rapidly when $[Te^{2-}]$ / $[CdCl_2]$ < 0.2. This phenomenon can be related to the reason of over passivation of the surface of the QDs, which lead to screwy surface that gave rise to new nonradiative defects.[1,4]

The reaction temperature and time significant influence the spectral properties of as-prepared QDs. In the previous report, the QDs prepared in the aqueous phase with NIR region are usually possessed poor spectral properties such as low PLQYs and broad FWHM than those in the blue and visible regions.[5,6] This phenomenon can be related to two factors: the property of component material and improper reaction temperature and time.[6] Compared to conventional thermal techniques, microwave methodology has many dominating merits such as easy heat control, high reaction selectivity and homogeneous heating. However, CdHgTe/CdS/CdZnS CSS QDs possess more complicated process of crystallization and a high degree of surface disorder of crystal nuclei than CdHgTe QDs.[7] Thus, we herein choose program process of microwave irradiation to control the accurate temperature of nucleation and epitaxial-type shell growth for CdHgTe/CdS QDs.[2,8,9] Than, a CdZnS shell was epitaxially overcoated around the outer layer of the core/shell QDs without any purification. The reaction temperature and time played important role in the formation of CdZnS shell on the core/shell QDs. As shown in Figure 2b， the optimum temperature to form NAC capped CdHgTe/CdS/CdZnS QDs is 90°C during the formation of the CdZnS shell on the CdHgTe/CdS core/shell QDs. The formation of the CdZnS shell structure can passivity the surface of the CdHgTe/CdS QDs and reduce their band gap, resulting in the red shift of both first absorption peak and PL emission peak.[1,9] The optimum temperature for MPA capped CdHgTe/CdS /CdZnS QDs and TGA-capped CdHgTe/CdS/CdZnS QDs were 90 °C and 75 °C, respectively. The results indicated TGA was more likely to be prone to thermal decomposition than other ligands. Lower reaction temperature would decrease the growth speed and adversely influence the quality of the QDs. On the contrary, higher reaction temperature cause detachment of the excessive ligands from CdHgTe surface, which results in large amount of surface defects and an obvious decline of PLQYs.[3,10,11] It is worth mentioning, however, the reaction time of our method is much lesser in contrast to some reported which synthesis of NIR-emitting QDs in aqueous solutions that took several hours or even days (figure 2c).[8,12] The reason is that the kinetics of the reaction rate are increased by 1-2 orders of magnitude by using microwave dielectric heating.[11] When the reaction time was prolong to 40 min, excessive energy cause excessive decomposition of thiols and an increase in the formation rate of complexes, which results in new hot spots where nonradiative recombination take place and an obvious decline of PLQYs.

The value of pH also plays an important role in affects the quality of as-prepared QDs.[3] Due to the excellent water-solubility in acidic, neutral, or alkaline medium, Cd-NAC complexes did not produce any white precipitates at pH 2.4-12. [3] When MPA was used as the stabilizer, the initial mixtures of Cd-MPA are insoluble at pH lower than 7.3. In the investigation of the pH effect, we changed the pH value from the most often used 6.0 to 7.0, 8.0, 8.5, 9.0, 9.5, 10.0, 11.0, and 12.0. Fig. S2d shows the evolution of the PLQYs of CdHgTe/CdS /CdZnS QDs prepared at different pH values. It clearly indicates that with the increase of pH value from 8.0 to 9.5, the PLQYs of CdHgTe/CdS /CdZnS QDs changed inconspicuous. At this range, TGA-capped QDs exhibit lower PLQYs in low pH values solution. When the pH value changed from 9.5 to 12, the curves of PLQYs fluctuate obviously. It should be noted that lower pH was possibly attributed to the formation of the thicker shell on particles surface for NAC or MPA, which not only decreased the traps on QDs surface, but also acted as a factor to form core/shell structure.[13]

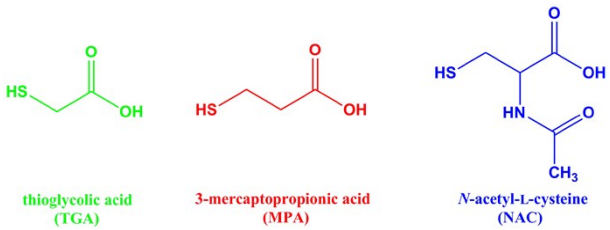

Fig. S2 Chemical structures of the ligands used.

RSC Advances

SUPPORTING INFORMATION

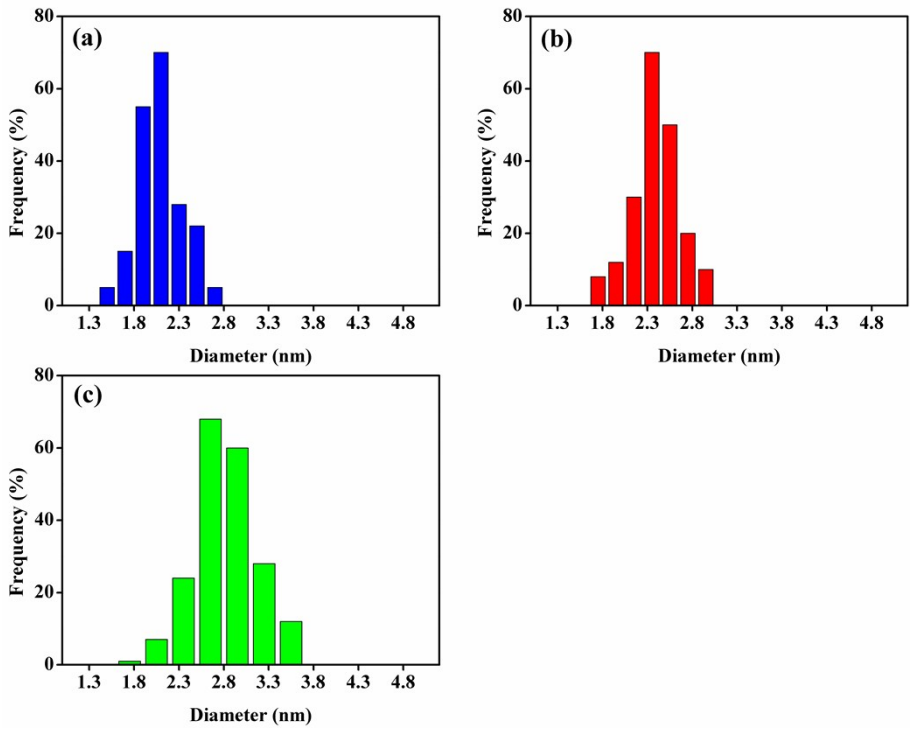

Fig. S3 Histograms of the size distribution of CdHgTe/CdS/CdZnS QDs capped by NAC (a), MPA (b) and TGA (c) , respectively.

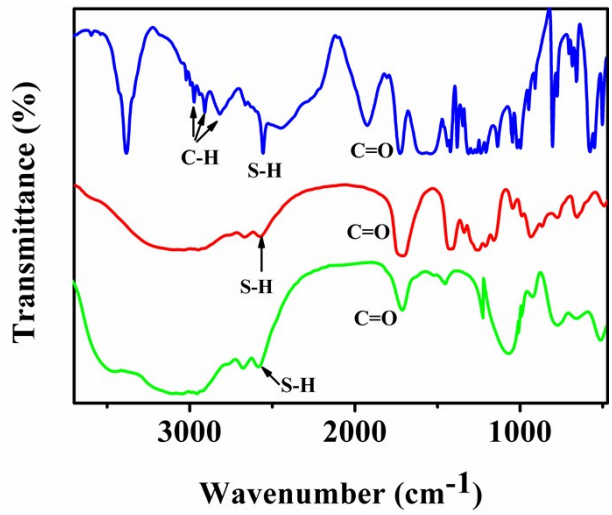

Fig. S4 FT-IR absorption spectra of NAC (blue), MPA (red) and TGA (green), respectively.

Fig. S4 represents the Fourier Transform Infrared Spectroscopy (FT-IR) spectra of NAC (blue), MPA (red) and TGA (green), respectively. The C=O band at 1716 cm^{-1} were shifted to the COO^- band at 1558 cm^{-1}. For the spectrum of NAC, the characteristic peaks at 2982, 2907 and 2800 cm^{-1} is corresponding to S–H stretching vibration.

Stability of CdHgTe/CdS/CdZnS QDs

Before measurement, the samples were washed with ultrapure water three times to remove any residual reagent and the achieved precipitates were re-dissolved (A=0.1) in Milli-Q water. For storage stability, the achieved precipitates were re-dissolved (A=0.1) in Milli-Q water and stored in dark. The photostability of aqueous dispersions of CdHgTe/CdS/CdZnS QDs was studied by irradiating the samples with a 200 W xenon lamp at 365nm under open air condition at room temperature. The samples were washed with ultrapure water three times to remove any residual reagent and the achieved precipitates were re-dissolved (A=0.1) in Milli-Q water before measurement. The distance between the sample solutions and lamp was fixed to 5 cm. Aliquots of the sample solution were taken at regular intervals for PL measurements. The fluorescence quenching of BSA by CdHgTe/CdS/CdZnS QDs was studied by spectrofluorometry at room temperature. The stock solution of BSA was dissolved in PBS buffer solution (0.01M, pH=7.2).When the BSA solution (1.0×10^{-6} M) were manually titrated into the QDs solution (3 mL). The PL intensity was measured at regular intervals. During the oxidation stability etching experiments, 3 % H_2O_2 (0.025 mL) solution was added to the QDs solution (3.0 mL) with stirring under ambient conditions at room temperature. The PL intensity was recorded after different intervals of etching time.

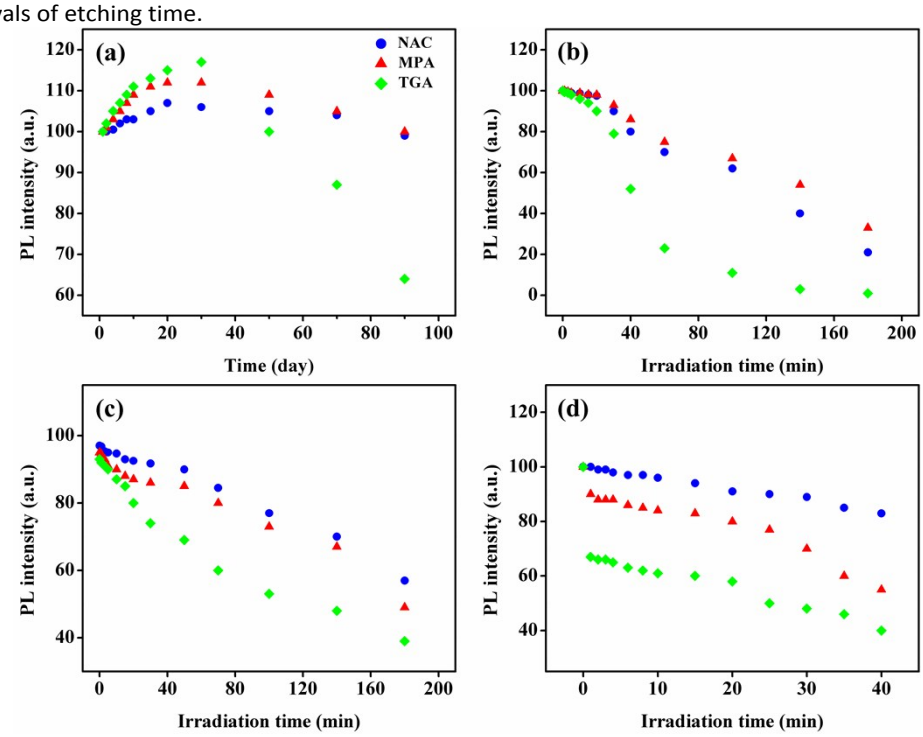

Fig. S5 (a) PL intensity evolution of the QDs over three months in aqueous solution. Photostability experiments of the as-prepared QDs in aqueous solution (b) and BSA solution (c). (d) Oxidative stability experiments of CdHgTe/CdS/CdZnS QDs. For all samples, emission features of selected NAC (blue), MPA (red) and TGA (green) capped CdHgTe/CdS/CdZnS QDs, respectively.

The stability of QDs is critically important for biological applications.[14] Bare CdHgTe QDs easily degradation during storage, the stability of as-prepared QDs further raised by constructing double shells structure around the core.[5,14] The as-prepared NIR-emitting CSS QDs display superior storage ability. The PLQYs of MPA-or NAC-capped CSS QDs in aqueous solution slightly increased after storage for 20 days, then gradually decreased to the original intensity after storage for 90 days (Fig. S5a). Specifically, the PLQYs of the TGA-capped CSS QDs increased during the 30 days of storage, then farther decreased to the 64% of the original intensity after storage for 90 days (Fig. S5a). To further define the photostability of the prepared QDs, solutions with the QDs in ambient conditions were continuously irradiated by a 200W xenon lamp at 365 nm and their emission intensities were monitored over a period of 3h. Fig. S5b shows that the FL intensity of the TGA-capped QDs rapidly dropped to only 50% of the original fluorescence intensity in merely 40 min, and became negligible after 100 min. In sharp contrast, MPA-capped CdHgTe/CdS/CdZnS CSS QDs possess much better performance and slightly decreased after irradiation for 40min. Furthermore, for NAC-capped CSS QDs, the PL intensity stabilized at about 70% of its initial value after irradiation for 1h, indicating the remarkably photostability. Fig. S5c exhibit the photostability of CSS QDs in the presence of BSA solution. The PLQYs slightly decreased after conjugated with BSA, reconfirming that there is the ground state complex formation between BSA and QDs.[15] The fluorescence intensity of NAC-capped QDs remained almost the same as the original value when irradiation time was extended to 60 min, suggesting the excellent stability of CSS QDs in biological environments.

The oxidant from environmental condition or living body makes the oxidation process happen. During the etching experiments, 3% H_2O_2 were chosen to react with QDs solution to investigate their antioxidant stability. As seen from Fig. S5d,

there was an obvious decrease in the PL intensity for the obtained CSS QDs capped by TGA immediately. After 30 min, the PL intensity of MPA-capped QDs showed the same result. Comparatively, there was no obvious change in the PL intensity for NAC-capped QDs, indicating the oxidation of H_2O_2 exhibited no erosion effect. The result indicating that the NAC have the miraculous ability of antioxidation, which further strengthened the stability of the CdHgTe/CdS/CdZnS CSS QDs from the etching of outer environmental factors.

Cytotoxicity experiments

Hela cells were cultured in DMEM, supplemented with 10% heat-inactivated fetal bovine serum at 37°C in the humidified atmosphere with 5% CO_2. Before experiments, the cells were seeded onto 96 well plates and then incubated for 24 h (about 80% confluence) at 37°C. Then, Cells were washed once with phosphate buffered saline (PBS) and cultured with medium containing different concentrations of as-prepared QDs. After incubated for 30 min or 48 h, the stained cells were rinsed with PBS three times, followed by adding 20 μL stock MTT (5 mg/mL), and incubated at 37°C for 4 h. The supernatant medium was carefully removed and 150 μL of DMSO was added. Then, the plates were placed in a shaker for 10 min to fully dissolve the purple formazan crystals. Absorbance was measured at 490 nm using a UV-Vis spectrophotometer. Cells incubated in the absence of QDs were used as a control.

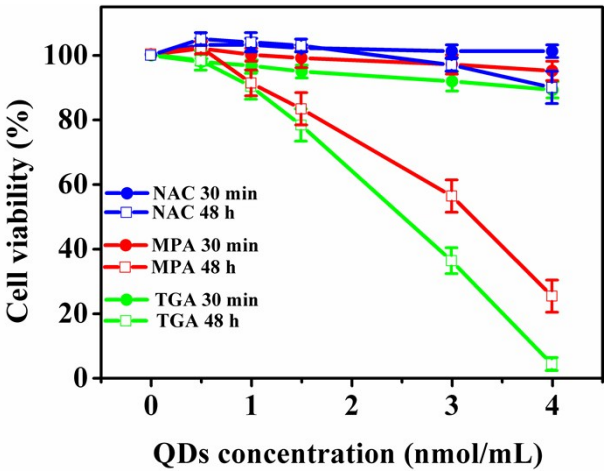

Fig. S6 Cell viability experiments using MTT assay for CdHgTe/CdS/CdZnS QDs capped by NAC (blue), MPA (red) and TGA (green) at different concentration.

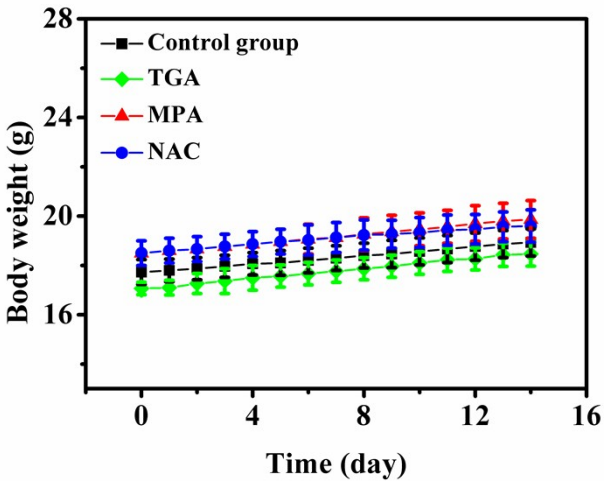

Fig. S7 Weights of mice were recorded after injection of the CdHgTe/CdS/CdZnS QDs capped by NAC (blue), MPA (red) and TGA (green).

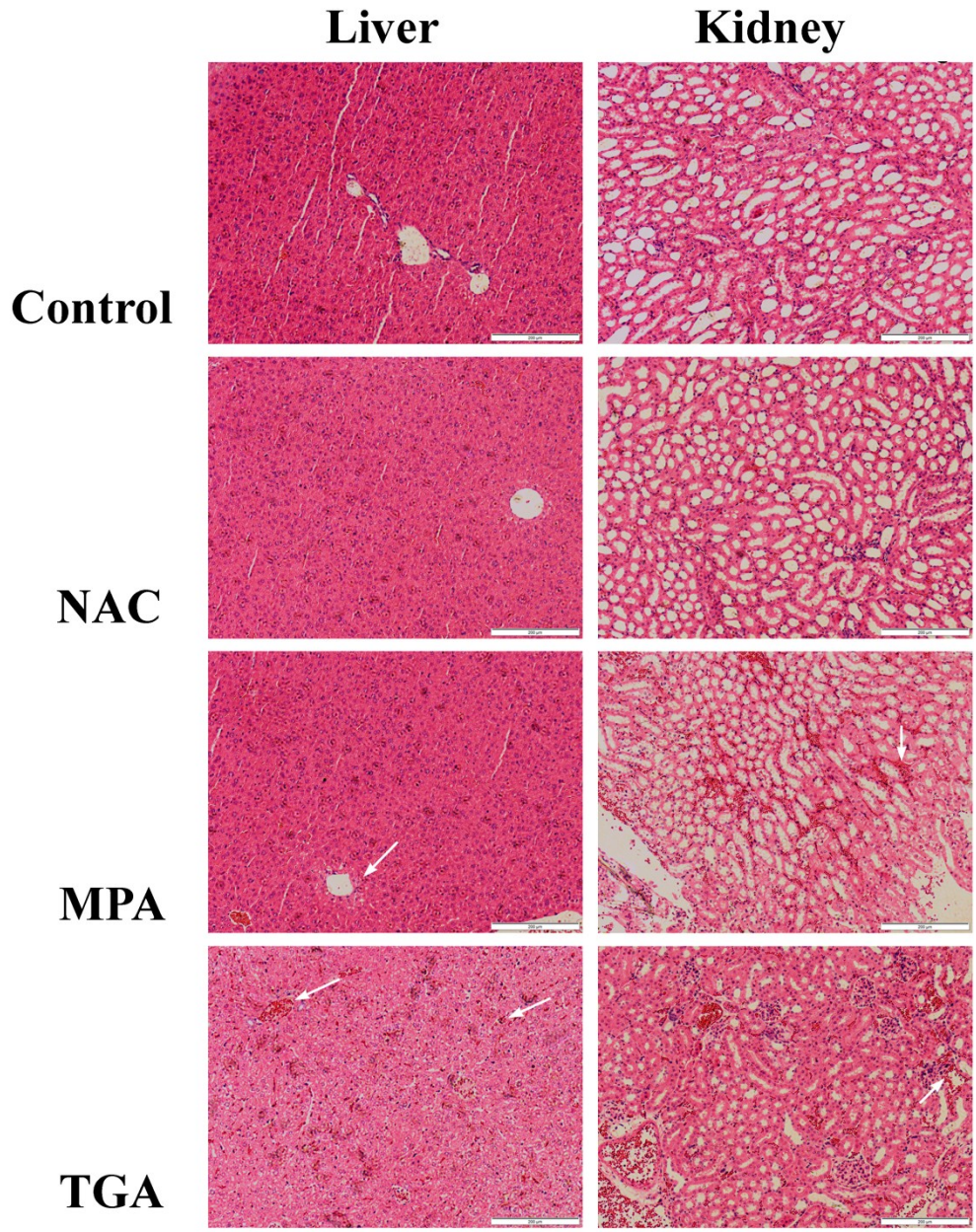

Fig. S8 Histological studies on the liver and kidney of the CdHgTe/CdS/ZnS QDs injected mice after 14 days. Scale bars are 200μm, respectively.

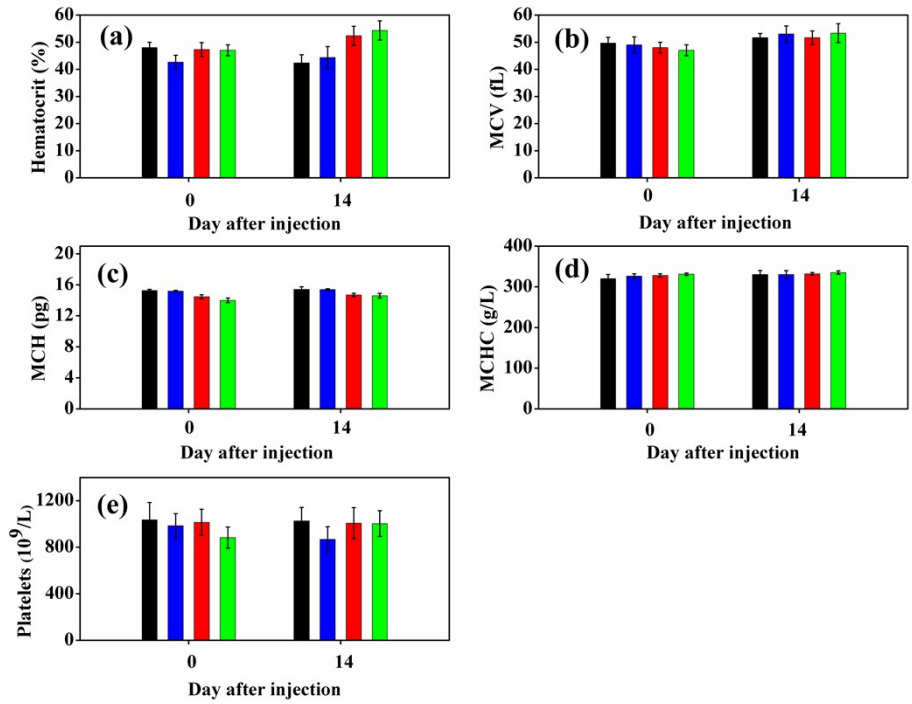

Fig. S9 Hematology results from mice treated with QDs of varying surface chemistry or a vehicle control (black). a–e) These results show mean and standard deviation of hematocrit (a), mean corpuscular volume, MCV (b), mean corpuscular hemoglobin, MCH (c), mean corpuscular hemoglobin concentration, MCHC (d), platelets (e). For all samples, parameters of selected NAC (blue), MPA (red) and TGA (green) capped CdHgTe/CdS/CdZnS QDs, respectively.

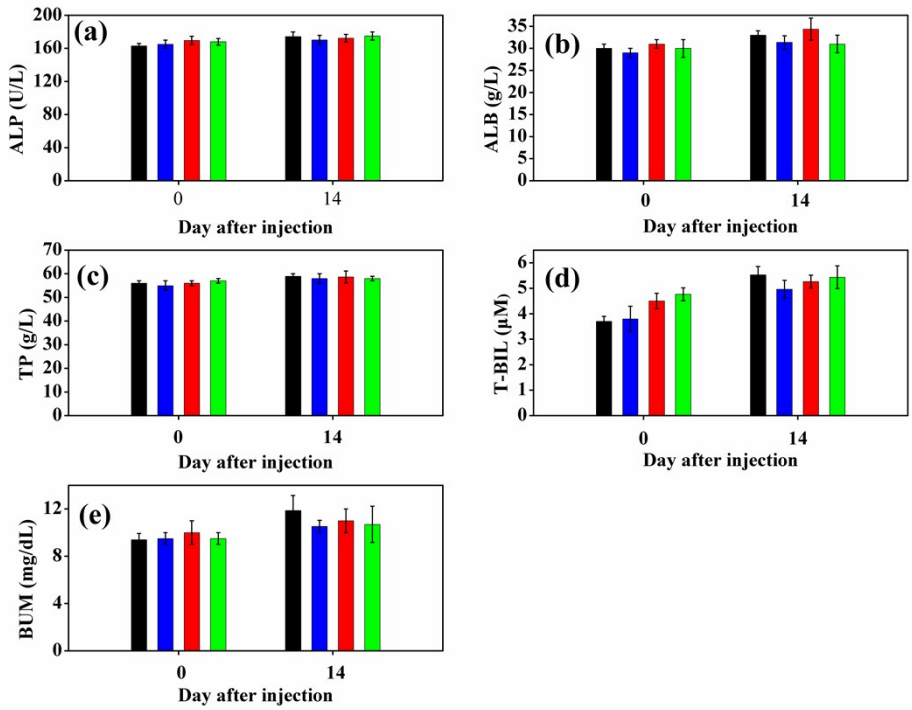

Fig. S10 Biochemistry results from mice treated with QDs of varying surface chemistry or a vehicle control (black). a–e) These results show mean and standard deviation of alkaline phosphatase, ALP (a), albumin, ALB (b), total bilirubin, T-BIL (c), total protein, TP (d), blood urine nitrogen, BUN (e). For all samples, parameters of selected NAC (blue), MPA (red) and TGA (green) capped CdHgTe/CdS/CdZnS QDs, respectively.

References

1 P. Reiss, M. Protière and L. Li, *Small*, 2009, **5**, 154 168.
2 X. J. Liu, P. J. Zhou, H. J. Zhan, H. Y. Liu, J. W. Zhang and Y. N. Zhao, *RSC Adv*., 2017, **7**, 29998 30007.
3 D. Zhao, Z. K. He, W. H. Chan and M. M. F. Choi, *J. Phys. Chem. C,* 2009, **113**, 1293 1300.
4 J. Wang, Y. T. Long, Y. L. Zhang, X. H. Zhong and L. Y. Zhu, *ChemPhysChem,* 2009, **10**, 680 685.
5 Y. He, Y. L. Zhong, Y. Y. Su, Y. M. Lu, Z. Y. Jiang, F. Peng, T. T. Xu, S. Su,Q. Huang, C. H. Fan and S. T. Lee, *Angew. Chem. Int. Ed.,* 2011, **50**, 5695 5698.
6 Q. Ma and X. G. SU, *Analyst,* 2010, **135**, 1867 1877.
7 W. J. Cai, L. M. Jiang, D. M. Yi, H. Z. Sun, H. T. Wei, H. Zhang, H. C. Sun and B, Yang, *Langmuir,* 2013, **29**, 4119 4127.
8 M. Q. Dai, W. Zheng, Z. Huang and L. Y. L. Yung, *J. Mater. Chem,* 2012, **22**, 16336 16345.
9 Y. He, H.T. Lu, L. M. Sai, W. Y. Lai, Q. L. Fan, L. H. Wang and W. Huang, *J. Phys. Chem. B*, 2006, **110**, 13352 13356.

10 A. Rogach, S. Kershaw, M. Burt, M. Harrison, A. Kornowski, A. Eychmüller and H. Weller, *Adv. Mater.,* 1999, **11**, 552 555.
11 Y. He, L. M. Sai, H.T. Lu, M. Hu, W. Y. Lai, Q. L. Fan, L. H. Wang and W. Huang, *Chem. Mater.,* 2007, **19**, 359 365.
12 H. F. Qian, C. Q. Dong, J. L. Peng, X. Qiu, Y. H. Xu and J. C. Ren, *J. Phys. Chem. C.,* 2007, **111**, 16852 16857.
13 L. Li, H. F. Qian, N. H. Fang and J. C. Ren, *J. Lumin.,* 2006, **116**, 59 66.
14 R. Gill, M. Zayats and I. Willmer, *Angew. Chem. Int. Ed.,* 2008, **47**, 7602 7625.
15 H. J. Zhan, P. J. Zhou, L. Ding, Z. Y. He and R. Ma, *J. Lumin.,* 2012, **132**, 2769 2774.